

# Depth Advanced Control of an Autonomous Underwater Robot

Hattab Abdellilah<sup>1</sup>, Yahiaoui Kamel<sup>1</sup>, Hattab Youcef<sup>2</sup>

<sup>1</sup> Automatic Department, Faculty of Electrical Engineering, University of Science and Technology, BP 1505, El Mnaouar, Bir El Djir 31000, Oran, Algeria. E-mail: hattab\_abdellilah@yahoo.fr

<sup>2</sup> Chemical Department, Faculty of chemical Engineering, University of Science and Technology, BP 1505, El Mnaouar, Bir El Djir 31000, Oran, Algeria.

---

This autonomous underwater robot control is a very challenging task because of autonomous underwater robot system nonlinearity, time-variance, uncertain external disturbance and difficulty in hydrodynamic modeling. Based on detailed autonomous underwater robot control survey and description of autonomous underwater robot dynamics, this paper proposes to introduce new control law algorithm based on high order sliding modes (HOSM) for depth control of the autonomous underwater robot. A comparison with classical sliding mode (SM) is carried out as well. These control techniques are based on second order sliding modes. High order methods allow overcoming the chattering effect by removing the discontinuity of the control vector. We show that these high order controllers hold the properties of classical SM control laws and remove chattering problem. Different simulations have been carried out to show the performance and effectiveness of the proposed method.

---

**Keywords:** *Autonomous underwater robots, control, High order sliding modes control, sliding modes control, mobile robot, depth control.*

---

© 2022 Published by Ainteliala

## 1. Introduction

Autonomous underwater vehicles (AUVs) are unmanned robotic platforms that can be preprogrammed to achieve accurate navigation, control, and guidance tasks. Nowadays, AUV (Autonomous Underwater Vehicle) are widely used military, commercial and scientific purpose, (J.M. Spiewak,2007). These:

- In the commercial field: The oil and gas industry uses AUVs to detailed maps of the seafloor before they start building subsea infrastructure; pipelines and subsea completions can be installed in the most cost effective manner with minimum disruption to the environment.
- In the military field: A typical military mission for an AUV is to map an area to determine if there are any mines, or to monitor a protected area (such as a harbor) for new unidentified objects. AUVs are also employed in anti-submarine warfare, to aid in the detection of manned submarines.
- In the scientific field: Scientists use AUVs to study lakes, the ocean, and the ocean floor. A variety of sensors can be affixed to AUVs to measure the concentration of various elements or compounds, the absorption or reflection of light, and the presence of microscopic life.

The navigation and the control of AUV are difficult and complex topics. The dynamics of AUV are highly nonlinear and depend on several parameters that are difficult to measure precisely (as the hydrodynamic coefficients, the added mass terms...). Therefore, the control law must be robust against the parametric uncertainties and the environmental perturbations acting on the vehicle.

The basic tasks in autonomous underwater systems are depth and steering control. A lot of control strategies have been adopted, all of them have advantages and disadvantages. It is possible to divide the algorithms in two groups: linear and nonlinear

In the linear methods: they are designed by using a vehicle's linear model, identified in a specific behavior case (nominal forward speed, angle of attack, etc.). These methods are **unable** to control easily a vehicle, but they work in specific conditions and model nonlinearities are non-considered. Some examples are PID control in (Jonghoon Park, 2000) and Linear Quadratic Gaussian LQG in (W. Naeem, 2003).

In the nonlinear methods: One of the most used methodologies in AUV control is the sliding mode control (SMC). For example the control of the NPS AUV by a typical SMC in (Marco, 2001) and an adaptive SMC in (Gianluca A, 2014), these strategies used linear vehicle's model in the nominal control. One example of SMC using a simplified nonlinear vehicle model for the nominal control is the AUV Marius (Fryxell, 1996). The main drawback of SMC is the Chattering effect that can excite unmolded high frequency modes, which degrades the performance of the system and may even lead to instability. Chattering also leads to high wear of fins and increase electrical power consumption. Other approach use full nonlinear model (Silvestre, 2007), here a Lyapunov and back stepping techniques are used in order to control the AUV Infante.

Sliding mode techniques are appropriate to underwater control, thanks to its robustness under parameters uncertainties. However chattering effect is its main disadvantage. In this paper, a recent method called HOSMC is implemented in AUV H160, in order to avoid the chattering problem and to improve control performance. High order techniques allow us to keep the main advantages of the classical SMC and to remove the chattering problem. The implementation of a second order sliding mode control in the AUV H160 using its simplified nonlinear model, is the main contribution of this paper.

The paper is organized as follows. Section 2 presents the kinematic and vertical dynamic models of the AUV. A second order sliding mode control structure used for the AUV is described in Section 3. Effectiveness of the proposed schemes is demonstrated by simulation in Section 4. Finally, the conclusion is given in Section 5.

## 1. Mathematical modeling

The equations of motion for underwater vehicles can be presented with respect to a Body-fixed frame relative to an Earth-fixed frame, Figure 1.

The position of the Body-fixed measured in the Earth-fixed is,

$$\eta = \begin{bmatrix} \eta_1 \\ \eta_2 \end{bmatrix}; \quad \eta_1 = \begin{bmatrix} x \\ y \\ z \end{bmatrix}; \quad \eta_2 = \begin{bmatrix} \phi \\ \theta \\ \psi \end{bmatrix} \quad (1)$$

$$v = \dot{\eta}$$

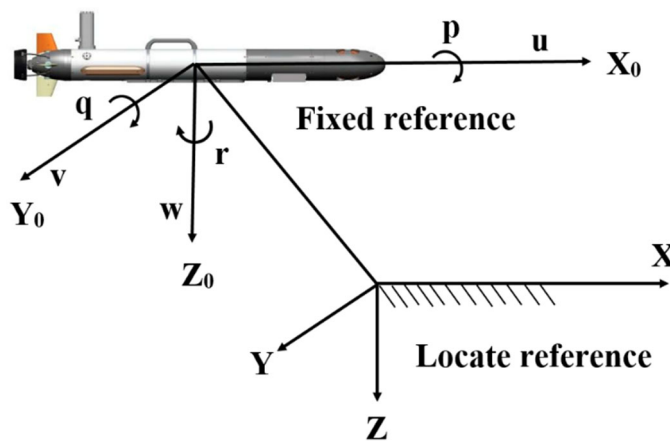


Figure 1. Reference marks representation

### A. Kinematics model

The vehicles-fixed linear and angular velocity and the time derivative of the earth-fixed vehicle position coordinates are related by the following relationships (Figure 2):

$$\begin{aligned} \dot{\eta} &= J_c(\eta_2) v \\ \begin{bmatrix} \dot{\eta}_1 \\ \dot{\eta}_2 \end{bmatrix} &= \begin{bmatrix} J_{c1}(\eta_2) & 0_{3 \times 3} \\ 0_{3 \times 3} & J_{c2}(\eta_2) \end{bmatrix} \begin{bmatrix} v_1 \\ v_2 \end{bmatrix} \end{aligned} \quad (2)$$

Where  $J_{c1}(\eta_2)$  is the transformation matrix of the linear velocity and  $J_{c2}(\eta_2)$  is the transformation matrix of the angular velocity. This representation has a singularity for  $\theta = \pm 90^\circ$ .

$$J_{c1}(\eta_2) = \begin{bmatrix} c\theta c\psi & s\theta s\phi c\psi - s\psi c\phi & s\theta c\phi c\psi + s\psi s\phi \\ c\theta s\psi & s\theta s\phi s\psi + c\phi c\psi & s\theta c\phi s\psi - c\psi s\phi \\ -s\theta & c\theta c\phi & c\theta s\phi \end{bmatrix} \quad (3)$$

$$J_{c2}(\eta_2) = \begin{bmatrix} 1 & s\phi t\theta & c\phi t\theta \\ 0 & c\phi & -s\phi \\ 0 & s\phi / c\theta & c\phi / c\theta \end{bmatrix}, \begin{cases} c = \cos \\ s = \sin \\ t = \tan \end{cases} \quad (4)$$

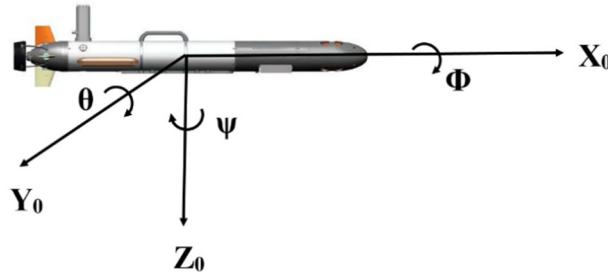


Figure 2. Definition of swing angles

### B. Dynamic model

The vehicle dynamics model derived by (SNAME, 1994) is based on a set of dynamic equations that govern the vehicle's translational and rotational motion in 3-D space. Using the Newton laws, the translational and rotational motions are:

$$\begin{cases} m^* \gamma = \sum F \\ I^* \ddot{\alpha} = \sum M \end{cases} \quad (5)$$

where  $F$  is the net external force applied to the vehicle,  $m$  is the mass of the vehicle,  $\gamma$  is the acceleration of its mass center with respect to an inertial frame,  $M$  is the net external moment acting on the vehicle at the center of mass,  $I$  is the inertia tensor about the vehicle's mass center, and  $\ddot{\alpha}$  is the vehicle's angular acceleration.

The external forces and moments on the vehicle are due to gravitational, buoyancy, propulsive, control and hydrodynamic effects. As shown by (T.Salgado. Jimenez, 2003), the motion equations given by (5) can also be written in the form:

$$M_{RB} \dot{v} + C_{RB}(v) v = \Gamma \quad (6)$$

Where  $M_{RB}$  is the inertia matrix including added mass, and  $C_{RB}(\nu)$  is a matrix that includes centrifugal and Coriolis forces.

$\nu$  is the generalized velocity vector in the body-fixed frame, and  $\dot{\nu}$  is the acceleration vector in the body-fixed frame. Generalized force vector  $\Gamma$  has the following components:

$$\Gamma = \Gamma_h + \Gamma_g + \Gamma_u + \Gamma_p \quad (7)$$

Where  $\Gamma_h$  present the hydrodynamics force vector of the vehicle body,  $\Gamma_g$  is the static force vector (gravity and buoyancy),  $\Gamma_u$  is the controlled force vector (include the thruster force and the fin force) and  $\Gamma_p$  is outside disturbances force and moment acting on the AUV.

### i) Hydrodynamic forces

In this section, we will discuss the hydrodynamic forces for AUV. The balance of efforts due to the inertia and mass of water added can be put in the form:

$$-(M_a \dot{\nu} + C_a(\nu)\nu) = \Gamma_a \quad (8)$$

Where  $M_a$  is the added mass matrix and  $C_a(\nu)$  is a Coriolis-like matrix

The viscous damping force is given by the damping matrix  $D(\nu)$  is given by

$$-D(\nu)\nu = \Gamma_d \quad (9)$$

With  $\Gamma_h = \Gamma_a + \Gamma_d$  is the vector of hydrodynamic efforts.

### ii) Hydrostatic forces

A solid body submerged in a fluid will have upward buoyant force acting on it equivalent to the weight of displaced fluid, enabling it to float or at least to appear to become lighter.

If the buoyancy exceeds the weight, then the object floats, if the weight exceeds the buoyancy, the object sinks. If the buoyancy equals the weight, the body has neutral buoyancy and may remain at its level. Discovery of the principle of buoyancy, which is a result of the hydrostatic pressure in the fluid, is attributed to Archimedes (figure 3).

Hydrostatic force includes the gravity part WW and the buoyancy part BB. The balance of hydrostatic efforts can be put in the form:

$$-g(\eta) = \Gamma_g \quad (10)$$

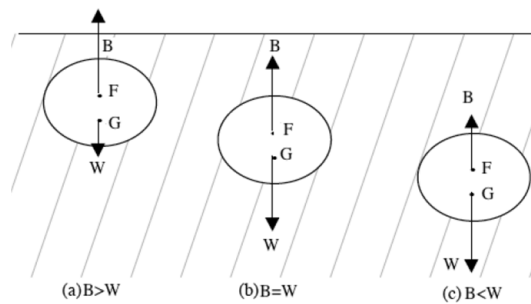


Figure 3. Hydrostatic equilibrium

### iii) Actuators of the robot

Actuators forces can be decomposed into lift and drag forces, perpendicular and parallel to the incoming fluid flow, respectively.

The control plane forces in the body frame, acting at the center of pressure of the control planes, are computed as:

When we use fins to control the motion of the AUV, the vehicle must maintain a surge speed. The propeller is used to generate energy to provide the surge force and then keep the vehicle moving ahead. Of course, the number of propellers mounted on the vehicle can be more than one. In the modeling process, we view the propeller as a special module and model it independently.

The thrust force generated by a propeller and (A. Crosnier, 2001) can compute the rolling moment caused by the propeller:

On the vertical control planes

$$\begin{bmatrix} F_x \\ F_z \\ M_q \end{bmatrix} = \begin{bmatrix} -0.5\rho S_s V_0^2 (C_{zs} \sin \delta_p + C_{xs} \cos \delta_p) \\ -0.5\rho S_s V_0^2 (C_{zs} \sin \delta_p - C_{xs} \cos \delta_p) \\ F_z (0.2c_s \cos \delta_p - d_{as}) + F_x (0.2c_s \sin \delta_p) \end{bmatrix} \quad (11)$$

On the horizontal control planes

$$\begin{bmatrix} F_x \\ F_y \\ N_r \end{bmatrix} = \begin{bmatrix} -0.5\rho S_s V_0^2 (C_{ys} \sin \delta_c + C_{xs} \cos \delta_c) \\ -0.5\rho S_s V_0^2 (C_{ys} \sin \delta_c - C_{xs} \cos \delta_c) \\ F_y (0.2c_s \cos \delta_c - d_{as}) + F_x (0.2c_s \sin \delta_c) \end{bmatrix} \quad (12)$$

Where  $\rho$  is the fluid density,  $S_s$  is the surface of the wing  $S_s = b_s \times c_s$ ,  $V_0$  is the modulus of the fluid flow around the wing,  $0.2c_s$  is the distance from the leading edge of the wing at its point of application of hydrodynamic forces,  $C_{ys}$  and  $C_{xs}$  represent the coefficients of lift and drag.

When we use fins to control the motion of the AUV, the vehicle must maintain a surge speed. The propeller is used to generate energy to provide the surge force and then keep the vehicle moving ahead. Of course, the number of propellers mounted on the vehicle can be more than one. In the modeling process, we view the propeller as a special module and model it independently.

The thrust force generated by a propeller and (A. Crosnier, 2001) can compute the rolling moment caused by the propeller:

$$T_p = \rho D_p^4 K_T (J_0) |n_p| n_p \quad (13)$$

$$Q = \rho D_p^5 K_Q (J_0) |n_p| n_p \quad (14)$$

Where  $n_p$  is rotating rate of the propeller,  $\rho$  is the fluid density,  $D_p$  is the propeller diameter,  $K_T$  is the thrust coefficient,  $K_Q$  is torque coefficient  $J_0 = V_a / (n_p D_p)$  is the advance number.  $V_a$  is the advance speed at the propeller (speed of the water going into the propeller) which has a relationship with surge velocity  $V_0$ :  $V_a = (1 - w_a) V_0$

Where  $w_a$  is the wake fraction number (typically: [0.1:0.4]).

The final dynamic equation of the robot is as follows (Bekit. B, 1997):

$$M\dot{v} + C(v)v + D(v)v + g(\eta) = \Gamma \quad (15)$$

Where

$M = M_{RB} + M_a$  is the inertia and added mass matrix,  $C(v) = C_{RB}(v) + C_a(v)$  is the matrix of Coriolis and centripetal forces, from inertia and hydrodynamics,  $D(v)$  is the hydrodynamic damping and  $g(\eta)$  is the vector of restoring forces and moments.  $\Gamma$  is control-input vector describing forces and moment efforts

$$\Gamma = [\delta_p, \delta_c, n] \quad (16)$$

With  $\delta_p$  is the fin angle of AUV,  $\delta_c$  is the rudder angle of AUV,  $n$  is the revolution of propeller as thrusters of AUV.

### B. General equation of motion

The nonlinear vehicle equation of motion is written as:

$$\begin{cases} \dot{\eta} = J_c(\eta_2)v \\ M\dot{v} + C(v)v + D(v)v + g(\eta) = \Gamma \end{cases} \quad (17)$$

Hence, the global state vector is represented by:

$$(\eta, v) = [x \ y \ z \ \phi \ \theta \ \psi \ u \ v \ w \ p \ q \ r]^T \quad (18)$$

### C. Depth plane model

In this article, we are interested to study the behavior of autonomous underwater robot in the depth plane, so we only need to position ( $z$ ), the pitch angle ( $\theta$ ), linear velocity ( $w$ ) and angular velocity ( $q$ ).

Then we considered the other variables states as null.

$$\begin{bmatrix} \dot{w} \\ \dot{q} \\ \dot{\theta} \\ \dot{z} \end{bmatrix} = \begin{bmatrix} -0.7234 & 0.2374 & 0 & 0 \\ 0.6398 & -2.1281 & -0.2478 & 0 \\ 0 & 1 & 0 & 0 \\ 1 & 0 & -1.8 & 0 \end{bmatrix} \begin{bmatrix} w \\ q \\ \theta \\ z \end{bmatrix} + \begin{bmatrix} -0.2858 \\ -1.8904 \\ 0 \\ 0 \end{bmatrix} \delta_p \quad (19)$$

## 2. Sliding mode controller

Nonlinear model based control systems offer a level of dynamic capabilities which linear techniques are incapable of providing when dealing with parameter uncertainties and unmodelled dynamics. Sliding mode (Edwards, 1998), is categorized as a variable structure control system which has excellent stability, robustness, and disturbance rejection characteristics. This type of control is not new to submarines, in fact it is widely used due to its capability to overcome modeling errors (due in this case to the hydrodynamic terms and modeling as an uncoupled system). Sliding mode has been used in spacecraft (Lo.S, 1995), robotics (Bekit. B, 1997), missiles (Edwards, 1998), and many other applications where modelling error is a concern.

The idea behind SMC is to define a surface along which the process can slide to its desired final value (Gamal A Elnasbar, 2014), (Mohammed Reza, 2015). The structure of the controller is intentionally altered as its state crosses the surface in accordance with a prescribed control law. The SMC control law consists of two additive parts. That is:

$$u = u_{eq} + u_{glis} \quad (20)$$

Where

$u_{eq}$  : Nominal control, which is determined by the robot model.

$u_{glis}$  : Sliding part, which is useful to compensate model uncertainties.

Sliding surface in the state error space for tracking problem is defined and now the state errors are:

$$\tilde{x} = x - x_d \Rightarrow \begin{bmatrix} \tilde{w} \\ \tilde{q} \\ \tilde{\theta} \\ \tilde{z} \end{bmatrix} = \begin{bmatrix} w - w_d \\ q - q_d \\ \theta - \theta_d \\ z - z_d \end{bmatrix} \quad (21)$$

Where  $x_d$  desired tracking state. Now, sliding surface can be defined in the error state space form as follows

$$s = [\alpha \quad \beta \quad \gamma \quad \mu] \begin{bmatrix} \tilde{w} \\ \tilde{q} \\ \tilde{\theta} \\ \tilde{z} \end{bmatrix} = S\tilde{x} \quad (22)$$

Where  $\alpha, \beta, \gamma$  and  $\mu$  are the sliding surface constants. The sliding surface  $s$  must obey the next condition:

$S$  is chosen so that  $\lim_{x \rightarrow \infty} \dot{s} \rightarrow 0$  and  $\lim_{x \rightarrow \infty} s \rightarrow 0$ , assure the convergence of the error state space  $\lim_{x \rightarrow \infty} \tilde{x} \rightarrow 0$ . The Lyapunov candidate function  $V(s) = \frac{1}{2}s^2$ , represents the decay of the energy's system, and guaranteed that the system state converge to the sliding surface if the following sliding condition is respected (Xueli wu, 2014):

$$\dot{V}(s) = s\dot{s} \leq -\eta|s| \quad (23)$$

Or,

$$\dot{s} \leq -\eta^2 \text{sign}(s) \quad (24)$$

Differentiating the sliding surface (22), we obtain:

$$\dot{s} = S^T \dot{\tilde{x}} = S^T (Ax + Bu - \dot{x}_d) \leq -\eta^2 \text{sign}(s) \quad (25)$$

The sliding surface time derivative permits to express the two parts of the control:  $u_{eq}$ , and  $u_{glis}$ , with

$$u = -(S^T B)^{-1} S^T Ax - (S^T B)^{-1} S^T \dot{x}_d - (S^T B)^{-1} \eta^2 \text{sign}(s) \quad (26)$$

Then, the control to apply to the system is deduced:

$$\begin{aligned} u &\leq u_{eq} + u_{glis} \\ u_{eq} &= -(S^T B)^{-1} S^T Ax - (S^T B)^{-1} S^T \dot{x}_d \\ u_{glis} &= -(S^T B)^{-1} \eta^2 \text{sign}(s) \end{aligned} \quad (27)$$

In our case, the desired states are constant values, so  $\dot{x}_d = 0$ . thus (27) becomes:

$$\begin{aligned} u &\leq u_{eq} + u_{glis} \\ u_{eq} &= -(S^T B)^{-1} S^T Ax = -kx \\ u_{glis} &= -(S^T B)^{-1} \eta^2 \text{sign}(s) \end{aligned} \quad (28)$$

The nominal control  $u_{eq}$  is calculated for  $s = 0$ , that is to say when the system is on the sliding surface. So, the feedback gain vector  $k$  is calculated to place the eigenvalues of the closed loop system in  $[\lambda_1 \quad \lambda_2 \quad \dots \quad \lambda_{n-1} \quad 0]$ , to have the desired dynamic in the sliding surface.

Thus, the robot linear model (19) becomes:

$$\dot{x} = Ax + Bu_{eq} = (A - Bk)x = A_c x \quad (29)$$

With  $A_c$ , the closed loop state matrix.

The sliding surface coefficients  $S$  are calculated to have  $\dot{s} = 0$ , so (25) becomes:

$$\dot{s} = S^T \dot{\hat{x}} = S^T \dot{x} = S^T A_c x = 0 \quad (30)$$

A solution of (30) is:

$$S^T A_c = A_c^T S = [0] \quad (31)$$

Therefore,  $S$  is the eigenvector of  $A_c^T$  associate to the null eigenvalue

Finally, the sliding surface and the command are given by the expression:

$$u = -(-0.3525w + 0.6095q - 0.0037\theta) - 0.25 \text{sign}(w - 4.9066q - 5.1998\theta + 0.6941(z - z_d)) \quad (32)$$

In the standard SMC, is discontinuous; this is the main reason why high frequency switching appears in the output signal (chattering effect), which causes problems in practical application. In order to avoid chattering, a high order sliding control is used (V.Creuze, 2002; J.M.Spiewak, 2007). HOSMC acts on the higher order time derivative of the system deviation, instead of influencing the first deviation derivative as it happens in SMC (A.Crosnier, 2001). Its principal characteristic is that it keeps the main advantages of the SMC, removing the chattering effects. The sliding order is a number of continuous total derivatives of approximately the sliding mode (Figure 4)

The proposed second order sliding mode control can be used as an alternative natural approach for smoothing the input signal. The sliding order is a measure of the degree of smoothness of the sliding variable approximately the sliding mode. This proposed technique can be considered an extension of the first order-sliding regime. It is composed of two parts (Manjusha bhav, 2015), (Sandeep kaur, 2014):

$$u = \int u_{eq} + K_{glis} \int u_{glis} \quad (33)$$

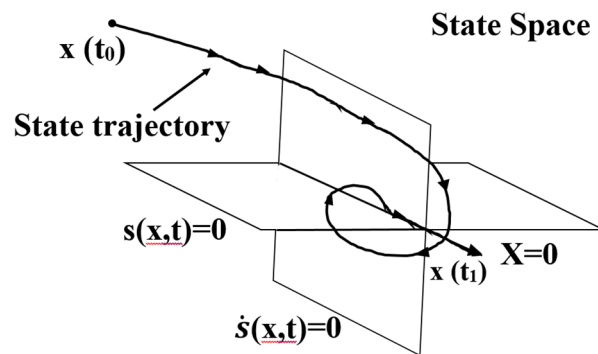


Figure 4. Second order sliding mode trajectory

$\int u_{glis}$  is composed of the integral of the function sign multiplied by a constant  $K_{glis}$ .

$\int u_{eq}$  is designed by using the equivalent command method for the new sliding surface  $s$ .

It is necessary to express the previous system (23) to appear the derivative of the control output



$$\begin{bmatrix} \dot{w} \\ \dot{q} \\ \dot{\theta} \\ \dot{z} \\ \dot{w} \\ \dot{q} \\ \dot{z} \end{bmatrix} = \begin{bmatrix} 0 & 0 & 0 & 0 & 1 & 0 & 0 \\ 0 & 0 & 0 & 0 & 0 & 1 & 0 \\ 0 & 1 & 0 & 0 & 0 & 0 & 0 \\ 0 & 0 & 0 & 0 & 0 & 0 & 1 \\ 0 & 0 & 0 & 0 & -0.7234 & 0.2374 & 0 \\ 0 & -0.2478 & 0 & 0 & 0.6398 & -2.1281 & 0 \\ 0 & -1.8 & 0 & 0 & 1 & 0 & 0 \end{bmatrix} \begin{bmatrix} w \\ q \\ \theta \\ z \\ \dot{w} \\ \dot{q} \\ \dot{z} \end{bmatrix} + \begin{bmatrix} 0 \\ 0 \\ 0 \\ 0 \\ -0.2858 \\ -1.8904 \\ 0 \end{bmatrix} \dot{\delta}_p \quad (34)$$

The new sliding surface is defined as follows:

$$\begin{aligned} s_p &= \dot{s} + \lambda s \\ &= \alpha \dot{w} + \beta \dot{q} + \alpha \lambda w + (\gamma + \beta \lambda) q + \gamma \lambda \theta + \mu \lambda \ddot{z} \end{aligned} \quad (35)$$

The equivalent command for the second order sliding technique is defined as follows:

$$u_{eq} = 0.2412 \dot{w} - 0.0637 \dot{q} + 0.5822 \dot{\theta} + 0.6941 \dot{z} \quad (36)$$

Finally, the command output is written:

$$\begin{aligned} \dot{\delta}_p &= 0.2412 \dot{w} - 0.0637 \dot{q} + 0.5822 \dot{\theta} + 0.6941 \dot{z} \\ &- 0.25 \text{sign}(\dot{w} - 4.9066 \dot{q} + 0.6941 \dot{z} + w - 10.1064 * q - 5.1998 \theta + 0.6941(z - z_d)) \end{aligned} \quad (37)$$

### 3. Simulation results

In this section, numerical simulations in the AUV hydrodynamic simulator are presented. It is a small size and low cost torpedo-shape AUV, used in very shallow water applications. Its dimensions are 1.9 m of length, a diameter of 0.25 m and a weight of 40 kg (for more details see (J.M.Spiewak, 2007)).

In the simulation, the following initial conditions are reconsidered:

- The desired outputs are position steps;  $z_d = 10.0 \text{ m}$  and  $\theta_d = 0.0^\circ$
- We consider that the vehicle is on the surface  $z_0 = 0.0 \text{ m}$  and the pitch angle is  $\theta_0 = 0.0^\circ$
- The AUV surge is constant:  $u = u_0 = 1.5 \text{ m/s}$

In numerical simulations, we add noise on each hydro-dynamic coefficient to simulate model's uncertainties. Moreover, we use a sea current to simulate environmental disturbances.

The robot reaches its desired depth  $z_d$  in 15s approximately (figure 5) with a zero pitch angle  $\theta = 0^\circ$  (figure 6). Indeed, as long as the desired depth  $z_d$  is not reached, the control surfaces are saturated (figure 7).

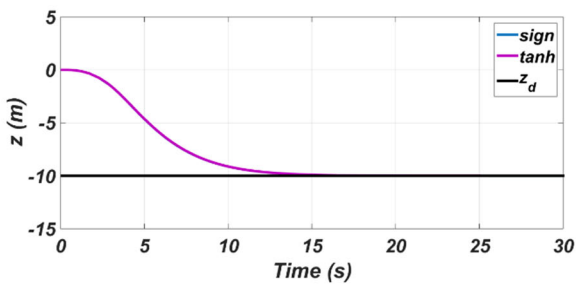


Figure 5. Depth control of robot with SMC

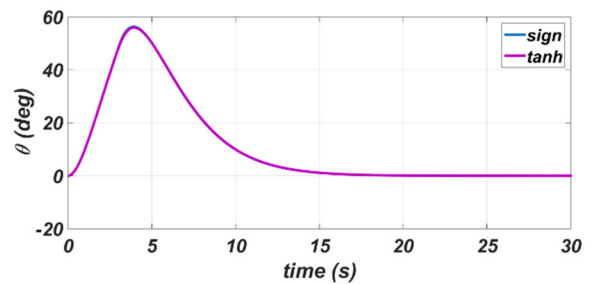
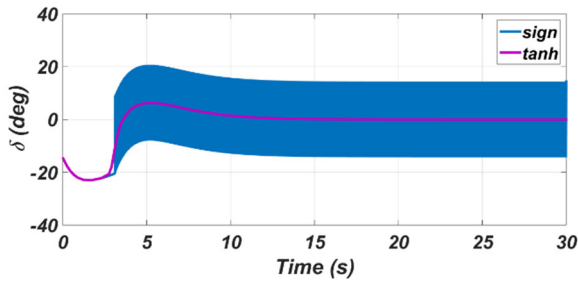
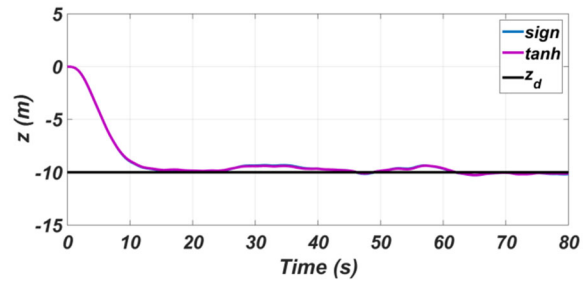


Figure 6. Pitch angle of robot with SMC

We can note in Figures (8-10), that the desired values are reached in spite of the sea current, of the parameters uncertainties and of the simplified linear model. The robustness of the SMC is due to the hard request of the rudders. The continual motion of the rudders is called, the chattering effect, and is due to the  $\dot{s}$  discontinuities. The chattering effect could excite the torpedo's own modes and damage the system. Moreover, the chattering effect causes an over consumption of energy.



**Figure 7.** Rudder control of the depth with SMC



**Figure 8.** Depth control of robot with SMC in disturbed

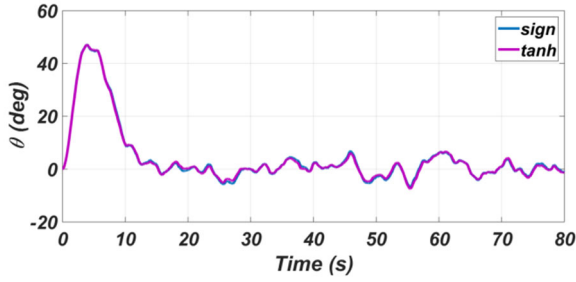


**Figure 9 .** Pitch angle of robot with SMC in disturbed environment.

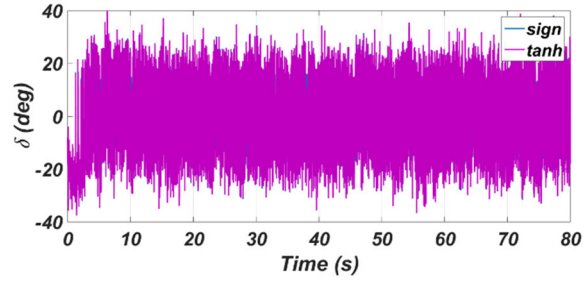


**Figure 10.** Rudder control of the depth with SMC in disturbed environment

A solution to limit this drawback is to replace  $\text{sign}(s)$  by  $\tanh\left(\frac{s}{\phi}\right)$ . The  $\phi$  parameter allows setting the boundary layer thickness. Figure 7 shows the results for the sign function and for the hyperbolic tangent function. However, this solution is not optimal owing to the fact that the system loses local robustness and that chattering reappears when the noise of the sensors is added with simulations (figure 10). Another solution to avoid the chattering effect is to use a high order sliding mode control.

The robot reaches its desired depth  $z_d$  in 17s approximately (figure 11), with the high order sliding mode control method.

We can see in Figure (12-16), the numerical simulation's results. With this control law, the amplitude of the chattering effect is reduced. In practice (figure 13, figure 16),  $\dot{s}$  can be unobservable, so its sign can be estimated by the sign of the first difference of the available sliding variable  $s$  in a time interval  $\Delta t$ .

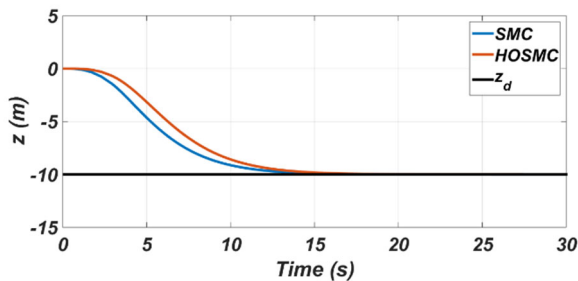


**Figure 11.** Depth control of robot with HOSMC

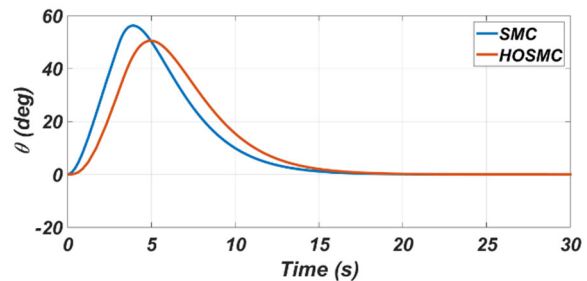


**Figure 12.** Pitch angle of robot with HOSMC

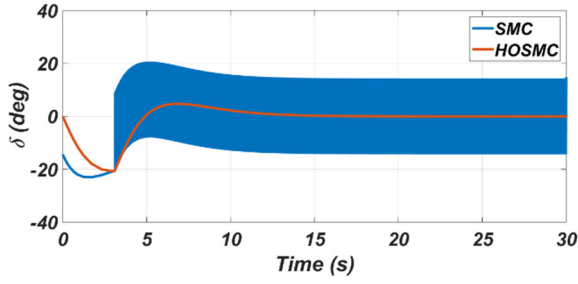


**Figure 13 .** Rudder control of the depth with HOSMC

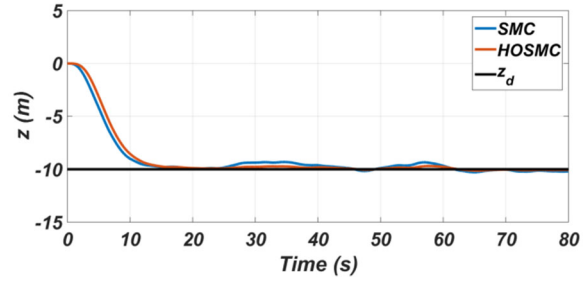


**Figure 14.** Depth control of robot with HOSMC in disturbed environment

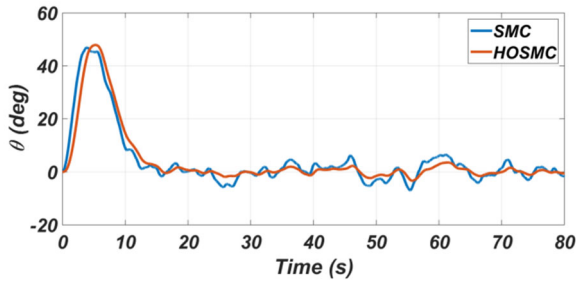


**Figure 15.** Pitch angle of robot with HOSMC in disturbed environment

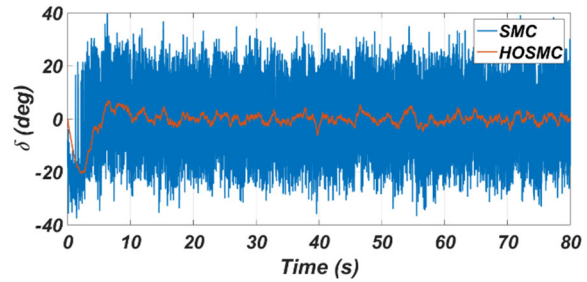


**Figure 16.** Rudder control of the depth with HOSMC in disturbed environment

#### 4. Conclusion

In this paper, we describe the robust control design laws methodologies, based on a simplified linear model of the autonomous underwater vehicle. Both simple and the high order sliding mode control are proposed and using in numerical simulations to control depth of autonomous underwater.

We can note that the SMC with the sign function consumes a lot. The use of hyperbolic tangent function instead of the signe in the simple sliding mode control reduces considerably the chattering effect. With the added sensors noise, which is closer to a real application condition, we noticed the reappearance of the chattering effect in the sliding mode control signal using hyperbolic tangent function. So the chattering effect is not reduced and we have to find a solution to overtake this limitation.

The implementation of the high order sliding mode control of the autonomous underwater vehicle is the solution we suggest and the most interesting contribution of this paper. Taking into account of the derivative of the sliding surface in the calculated command, the system reaches the sliding surface more slowly, we thereby avoiding the chattering effect, although we added the sensor noises simulation.

Finally, the sea current and parameter uncertainty are rejected by the first and second order sliding mode control laws. We can conclude that HOSM controllers eliminates the chattering effect and improve the system's accuracy convergence towards its desired behavior despite the presence of disturbances in comparison with the SMC controllers. The HOSMC controllers give better performance.

As a future work: The real time experimentation.

The implementation of the high order techniques to the roll plane.

The implementation of the sliding-mode control third order to the vertical and horizontal plane.

The implementation of the fuzzy high order-sliding mode control ZHOSMC to the horizontal and vertical plane.

## REFERENCES

- [1] A. Crosnier, G. Abba, B. Jouvencel and R. Zapata, (2001) 'Ingénierie de la commande des systèmes, techniques de base', *Ellipses*.
- [2] Bekit B., Whidborne, J., and Seneviratne, L., (1997) 'Fuzzy Sliding Mode Control for a Robot Manipulator', *The 1997 IEEE International Symposium on Computational Intelligence in Robotics*
- [3] C. Silvestre, A. Pascoal, (2007) 'Depth control of the INFANTE AUV using gain-scheduled reduced order output feedback', *control engineering practice, Elsevier*.
- [4] D. Fryxell, P. Oliveira and all, (1996) 'Navigation ,guidance and control of AUV's: an application the MARIUs vehicle', *control engineering practice, volume 4, N 03, pp 401-409, Elsevier science*.
- [5] Edwards, Christopher and Spurgeon, Sarah K., (1998) 'Sliding Mode Control, Theory and Applications', *Taylor and Francis*.
- [6] Gamal A. Elnashar , (2014) 'Dynamics modelling, performance evaluation and stability analysis of an autonomous underwater vehicle', *International Journal of Modelling, Identification and Control, 2014 - Vol. 21, No.3, pp. 306 - 320*.
- [7] Gianluca Antonelli, (2014) 'underwater robots', *book, disciplines: computer science engineering and robotics, Spring*.
- [8] J.M. Spiwak, (2007) 'Contribution à la coordination de flottille de véhicules sous-marins autonomes', *Thesis of University Montpellier II*.
- [9] Jonghoon Park , Wankyun Chung , Junku Yuh, (2000), 'Nonlinear  $H_{\infty}$  optimal PID control of autonomous underwater vehicles', *Proceedings of the 2000 International Symposium on Underwater Technology, IEEE, 2000. Page 193-198*
- [10] Lo, S. and Chen, Y., (1995) 'Smooth Sliding-Mode Control for Spacecraft Attitude Tracking Maneuvers', *Journal of Guidance, Control, and Dynamics, Vol. 18, No. 6, November-December 1995, pp. 1345-1348*.
- [11] Manjusha Bhawe, S. Janardhanan, Lillie Dewan , (2015) 'A smart higher order sliding mode control of rigid articulated robotic manipulator with passive joints', *Int. J. of Modelling, Identification and Control, 2015 - Vol. 23, No.3 pp. 260 - 266*.
- [12] Marco D.B, Healey AJ, (2001) 'Command, control and navigation experimental results with the NPS Aries AUV', *journal of oceanic engineering, IEEE, volume 26, ISSUE: 4, pp 466-476*.
- [13] Mohammad Reza Zarrabi, Mohammad Hadi Farahi, Sohrab Effati, Ali J. Koshkouei, (2015) 'Measure theory approach in sliding mode control for nonlinear systems with disturbances', *Int. J. of Modelling, Identification and Control, 2015 - Vol. 24, No.2 pp. 120 - 126*
- [14] Sandeep Kaur, S. Janardhanan, (2014) 'Second order sliding mode controller and online path planning for space rovers', *International Journal of Modelling, Identification and Control, 2014 - Vol. 21, No.3 pp. 321 - 329*
- [15] SNAME, (1994) 'Nomenclature for treating the motion of a submerged body through a fluid', *Technical Report No. I-5, Technical and research bulletin of the Society of Naval Architects and Marine Engineers, New York*.
- [16] T. Salgado-Jimenez, B. Jouvencel, (2003) 'Using high order sliding modes for diving control a torpedo Autonomous Underwater Vehicle', *OCEANS 2003, San Diego, USA, pp. 934-939*.
- [17] V. Creuze, (2002) 'Navigation référencée terrain pour véhicule autonome sous-marin', *Thesis of University Montpellier II, 2002*.
- [18] W. Naeem, R. Sutton and S. M. Ahmad, (2003), 'LQG/LTR Control of an Autonomous Underwater Vehicle Using a Hybrid Guidance Law', *Marine and Industrial Dynamic Analysis Group Department of Mechanical and Marine Engineering The University of Plymouth, PL4 8AA, UK, 2003*
- [19] Xueli Wu, Yang Li , Jianhua Zhang, Quanmin Zhu, (2014) 'Sliding mode control for neutral systems with uncertain parameters', *Int. J. Modelling, Identification and Control, Vol. 21, No. 1, 2014 , pp 65-71*.